

STABILITY DIAGRAMS FOR LANDAU DAMPING*

J. S. Berg[†], Brookhaven National Laboratory, Upton, NY, USA

Abstract

Stability diagrams allow one to determine whether a system is stable due to the presence of incoherent tune spread in a beam, a phenomenon known as Landau damping. This paper presents an overview of the mathematical foundations that underpin stability diagrams. I first describe stability diagrams as a mapping between two complex planes: the space of eigenvalues of the underlying Vlasov equation, and a space which can most easily be described as the product of beam current and an effective impedance. I go on to describe the circumstances when the Vlasov description of impedance-driven instabilities can or can not be formulated to construct a stability diagram. Finally I outline how this is applied to impedance-driven collective effects in particle accelerators.

INTRODUCTION

Stability diagrams allow one to determine whether a beam is stabilized by Landau damping by plotting the result of a relatively simple calculation involving the accelerator impedance and beam current on the same plane as a curve; the stability of the beam depends upon which side of the curve the point lies. The earliest use of stability diagrams was by Pease [1] for the case of longitudinal stability of unbunched beams. Several papers [2–4] expanded up on this with more examples and including the case of transverse stability of unbunched beams. Zotter [5] appears to be the first showing longitudinal bunched beam stability diagrams, and Chin [6] introduces transverse bunched beam stability diagrams.

The intention of this paper is to describe some mathematical foundations for the use of stability diagrams to calculate the point at which Landau damping is lost. I will describe the mathematics of the problem in terms of eigenmodes: complex (in the mathematical sense of “complex numbers”) distributions of particles that are invariant in all phase space variables except for the independent variable (for particle accelerations, often the length along a reference curve, but time for some applications). The dependence on the independent variable is exponential in the independent variable, with i times the coefficient being the eigenfrequency.

These eigenmodes can be divided into what are known as incoherent and coherent modes. Incoherent modes have a continuous spectrum for the eigenfrequency: the number of modes is uncountable (in the mathematical sense); the

spectrum is generally a union of intervals on the real line. Incoherent modes appear even in the absence of collective interactions. Their frequencies are the single particle frequencies we refer to as tunes, or multiples thereof. They have a spread in frequencies due to tune shift with amplitude, or chromaticity in the absence of longitudinal focusing. Their modes are distributions along a single line of constant action, and constant energy in the absence of longitudinal focusing.

The coherent modes have a discrete spectrum: there is a region in the complex plane around any mode in which there are only a finite number of modes. There are a countable (in the mathematical sense: the number could be infinite) number of such modes. These coherent modes are what one computes when the equations for collective effects are solved in the absence of tune shift with amplitude or chromaticity caused by the magnetic lattice or potential-well distortion.

In single particle dynamics, there is a phenomenon known as filamentation which is directly related to Landau damping. Imagine one starts with a distribution whose shape is not “matched” with the lines of constant amplitude. When there is a tune spread in amplitude, particles with different amplitudes rotate in phase at different rates, leading to a distribution which is effectively uniform in phase, without any particle actually changing its own amplitude. Simplistically, Landau damping occurs when the rate at which this filamentation occurs for the incoherent modes, which have real eigenvalues and therefore no change in their amplitude, is greater than the growth rate of the coherent modes.

For collective effects in particle accelerators, generally there is an intensity threshold below which the eigenvalue equation has no discrete modes: this is the mathematical manifestation of Landau damping. A stability diagram is a diagrammatic technique that can, for some restricted cases, allow one to quickly compute where this threshold lies. For cases where a stability diagram can be applied to a problem, one can plot the complex coherent mode frequencies in the absence of tune spread, or equivalently impedances, in the complex plane, and in the same plane draw a curve (the stability diagram); if the frequency lies on the inside the curve, the mode is said to be stabilized by Landau damping. In reality it is a statement that there is no such discrete mode.

GENERIC FORMULATION OF EIGENVALUE EQUATION

The equations describing the evolution of a distribution including collective effects can be Fourier transformed in the independent variable, and become an eigenvalue equation where the eigenvalue is the frequency corresponding to that independent variable. A generic form of the resulting

* This manuscript has been authored by employees of Brookhaven Science Associates, LLC under Contract No. DE-SC0012704 with the U.S. Department of Energy. The United States Government retains a non-exclusive, paid-up, irrevocable, world-wide license to publish or reproduce the published form of this manuscript, or allow others to do so, for United States Government purposes.

[†] jsberg@bnl.gov

eigenvalue equation is

$$[\Omega - \omega(x)]f(x) = \lambda \int K(x, \bar{x})f(\bar{x}) d\bar{x} \quad (1)$$

For particle accelerators: ω can be the tune (in which case x is an action variable) or an orbit frequency (x will be the energy); λ will be proportional to the beam current; K will be proportional to the impedance; and the phase space distribution will be contained in K . This description is very simplistic (in particular x can be a vector of variables, and these can be matrix equations), but sufficient for this initial discussion.

If $\omega(x)$ does not depend on x and K is sufficiently well-behaved, $f(x)$, the beam distribution in the frequency domain, can be written as a sum of coefficients times basis functions. The eigenvalue problem then becomes a linear algebra problem for the coefficients, with the matrix elements being integrals of products of K and the basis functions:

$$(\Omega - \omega)c_m = \lambda \sum_n Z_{mn}c_n \quad (2)$$

$$f(x) = \sum_k c_k B_k(x) \quad c_k = \int C_k^*(x)f(x) dx \quad (3)$$

$$Z_{mn} = \int C_m^*(x)K(x, \bar{x})B_n(x) dx d\bar{x} \quad (4)$$

A complete basis can be chosen so that the basis functions required to represent an arbitrary function is countably infinite. The resulting eigenvalue spectrum is also countably infinite but discrete. On formulating the linear algebra problem, one necessarily would take a finite number of basis functions, but as one increases the number of basis functions, the coefficients of the basis functions already included and their corresponding eigenvalues are expected to converge.

When $\omega(x)$ does depend on x , instead one develops a continuous, and therefore uncountably infinite, set of eigenvalue and eigenvectors for the problem. The eigenvalues in the continuous spectrum for Eq. (1) are just the range of $\omega(x)$, and therefore are real, for values of x where $K(x, \bar{x})$ is nonzero. The resulting eigenfunctions are not true functions but “distributions” [7]:

$$f_C(x, \Omega) = \delta(x - \omega^{-1}(\Omega)) + \text{PV} \frac{g(x, \Omega)}{x - \omega^{-1}(\Omega)} \quad (5)$$

$g(x, \Omega)$ can be computed by plugging f_C into Eq. (1) if so desired.

In addition, when $\omega(x)$ depends on x , there may still be a discrete eigenvalue spectrum with a countable number of eigenvalues as well, for which the eigenfunctions are non-singular ordinary functions. A generic distribution written in the domain of the independent variable (t here) will be a combination of the discrete and continuous modes:

$$f(x, t) = \int c(\Omega)f_C(x, \Omega)e^{-i\Omega t} d\Omega + \sum_n c_n f_{Dn}(x)e^{-i\Omega_n t} \quad (6)$$

For a sufficiently smooth $c(\Omega)$, the moments of $f(x, t)$, which lead to nonzero values on the right hand side of Eq. (1), that arise from the continuous part of Eq. (6) will decrease with time. Note that the coefficients in Eq. (6) are not changing in amplitude: particle amplitudes are not decreasing, only the moments that drive collective effects are. Any discrete modes (the second term in Eq. (6)) can still be exponentially increasing. However, for sufficiently small λ , there may not be any discrete modes: this disappearance of discrete modes is Landau damping.

GENERIC FORMULATION OF STABILITY DIAGRAMS

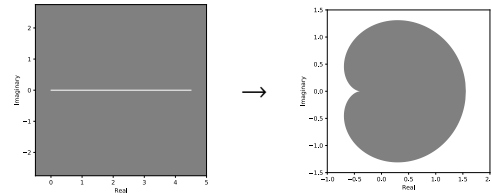
To determine when a system is “Landau damped,” one needs to find λ for which Eq. (1) has no discrete modes. The equation itself is not amenable to direct numerical solution due to the mixture of singular and non-singular modes and the uncountable eigenvalue spectrum. A stability diagram is an attempt to avoid this direct numerical simulation while still finding the λ for which the system has no discrete modes.

$f(x)$ can be expanded as a series of basis functions and Eq. (1) can be written similarly to Eqs. (2–4), but with $\Omega - \omega(x)$ moved to the side of the equation with $K(x, \bar{x})$:

$$c_m = \lambda \sum_n K_{mn}(\Omega)c_n \quad (7)$$

$$K_{mn}(\Omega) = \int \frac{C_m^*(x)K(x, \bar{x})B_n(\bar{x})}{\Omega - \omega(x)} dx d\bar{x} \quad (8)$$

Consider the properties of the functions $K_{mn}(\Omega)$. $|K_{mn}(\Omega)| \sim O(|\Omega|^{-1})$ as $|\Omega| \rightarrow \infty$. $K_{mn}(\Omega)$ is defined everywhere except for the line where Ω is in the range of $\omega(x)$ for x real and $K(x, \bar{x})$ is nonzero. Thus $K_{mn}(\Omega)$ defines a mapping of the entire complex plane, except for that line, to a bounded region of the complex plane:

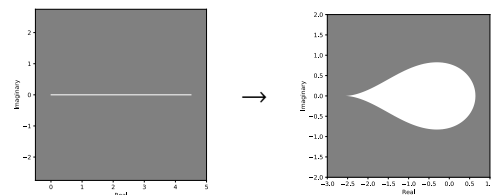


The boundary of the region can be found by evaluating $K_{mn}(\omega(x) \pm i\epsilon)$ for real x and infinitesimal ϵ .

Now consider a simplification of Eq. (7) where the matrix $K_{mn}(\Omega)$ is diagonal. Then the equation becomes

$$\lambda = 1/K_{mm}(\Omega) \quad (9)$$

The right hand side of Eq. (9) is a mapping of the complex Ω plane, except for the line mentioned above, to the complex plane with a hole in it:



Now consider the definition of $K_{mn}(\Omega)$ from Eq. (8), and assume that $\omega(x)$ did not depend on x ; then

$$K_{mn}(\Omega) = \frac{Z_{mn}}{\Omega - \omega} \quad (10)$$

where Z_{mn} is defined in Eq. (4). If $K_{mn}(\Omega)$ were diagonal, then Z_{mn} would be as well, in which case (if ω were constant), the equation for the eigenvalue Ω_0 would be

$$\Omega_0 - \omega = \lambda Z_{mn} \quad (11)$$

Combining Eq. (11) with Eq. (9), we have

$$\Omega_0 - \omega = \frac{Z_{mn}}{K_{mn}(\Omega)} \quad (12)$$

Equation 12 is the general form for any stability diagram, and indicates how a stability diagram is used. The eigenvalue equation is first solved without frequency spread (Eq. (11)), then the difference of the eigenvalue from ω is plotted in the same plane as the range of $Z_{mn}/K_{mn}(\Omega)$. In practice one plots the boundary $Z_{mn}/K_{mn}(\Omega \pm i\epsilon)$ for Ω real. If $\Omega_0 - \omega$ is outside the range of $Z_{mn}/K_{mn}(\Omega \pm i\epsilon)$ (i.e., on the origin side of the boundary), then such a solution cannot exist as a discrete mode: it is Landau damped. If $\Omega_0 - \omega$ is within the range of $Z_{mn}/K_{mn}(\Omega)$, then its frequency and growth rate can be determined by solving Eq. (12) for Ω . Note that $Z_{mn}/K_{mn}(\Omega) = \Omega + O(1)$ for large Ω .

If diagonalizing the problem is not acceptable, then one could start with the eigenvalue problem in Eq. (7), and treat it as an eigenvalue problem for λ^{-1} for fixed Ω . One can plot each eigenvalue as a function of $\Omega_0 \pm i\epsilon$ for Ω_0 real. That will give a closed curve for each eigenvalue; the region outside the closed curves for all of the eigenvalues is the region corresponding to values of λ that will result in no discrete eigenvalues for the original problem with Ω as the eigenvalue. λ will be a (possibly complex) constant times the beam current; taking a line along the appropriate direction in that region will allow one to determine the maximum current that is stable from Landau damping.

FORMULATION FOR PARTICLE ACCELERATORS

Now consider the accelerator problem. Equation (9) will usually (but not always) take the form

$$1 = -iC \frac{IZ_{\text{eff},m}}{E} \int \frac{\mathbf{m} \cdot \frac{\partial \psi_0}{\partial \mathbf{J}}}{\Omega - \mathbf{m} \cdot \boldsymbol{\omega}(\mathbf{J})} d\mathbf{J} \quad (13)$$

where I is the beam current, E is the beam energy, $Z_{\text{eff},m}$ an effective impedance (the impedance weighted by a function of frequency), and ψ_0 is a phase space distribution. $\boldsymbol{\omega}(\mathbf{J})$ can be a tune that varies with amplitude or an orbit period that varies with energy, or both. The phase space distribution is often Gaussian or a distribution that goes to zero reasonably smoothly at some number of σ [8, 9]. Using distributions with step truncations (“truncated Gaussian” distributions,

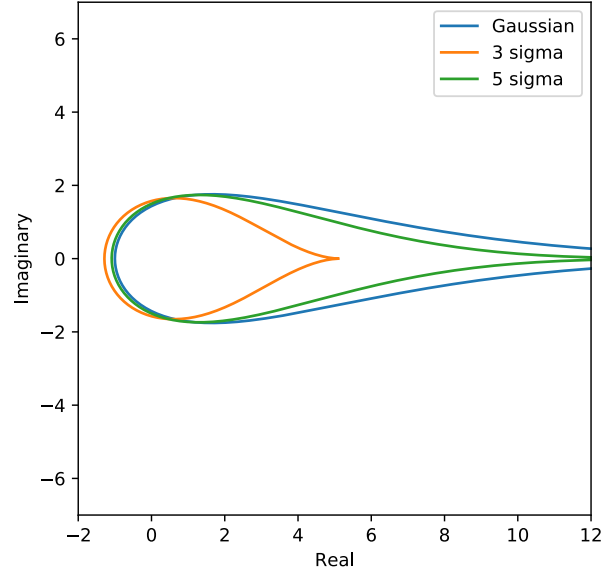


Figure 1: Stability diagrams for longitudinal motion and an unbunched beam. Different curves are for distributions smoothly truncated at a certain number of standard deviations, and a Gaussian distribution.

for instance) should be avoided for these computations, since one effectively picks up a discrete mode at the truncation (though collimation might make something similar occur).

Using Eq. (13) in Eq. (12), the impedance, current, and energy all disappear from the right hand side. Thus the stability diagram only depends on the phase space distribution ψ_0 and the mode m under consideration.

In the following subsections I outline the common cases for particle accelerators. These are meant only to summarize the characteristics of the behavior of these systems. I will leave out constants that do not serve to illustrate the points I am making. More detailed discussions are left to other references. I adopt the conventions of [9] for dimensionless functions used in constructing stability diagrams (Eqs. 14–17 are derived in detail there).

Longitudinal Impedance, Unbunched Beam

For a longitudinal impedance with no RF, the eigenvalue equation becomes

$$\frac{1}{\bar{B}_{\parallel} \left(\frac{k\omega_0 - \omega}{k\omega_0 \eta_c \sigma_{\delta}} \right)} = iC \frac{I}{E \eta_c \sigma_{\delta}^2} \frac{Z_{\parallel}(k\omega_0)}{k\omega_0} \quad (14)$$

B_{\parallel} is dimensionless, only depending on the shape (and not the scale) of the energy distribution in the beam. It’s behavior differs from what was described previously in that $1/B_{\parallel}(x)$ is proportional to x^2 , not x , for large x . Curves of $1/B_{\parallel}(x \pm i\epsilon)$ are plotted in Fig. 1 for both a Gaussian distribution and a distribution that goes smoothly to zero at 3 and 5 standard deviations [8, 9]. Note that the curve for $1/B_{\parallel}(x - i\epsilon)$ lies on top of the curve for $1/B_{\parallel}(x + i\epsilon)$; this behavior is unique

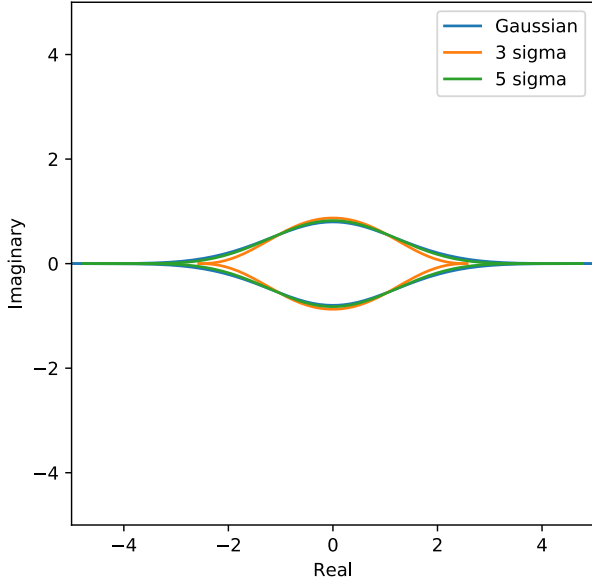


Figure 2: Stability diagrams for transverse motion and an unbunched beam where frequency spread arises from energy spread.

to the longitudinal unbunched case. To use this stability diagram, one plots the right hand side of Eq. (14) in the plane with the stability diagram; if the right hand side is inside the curve, then the mode is stable.

The longitudinal diagram gives the known behavior: the beam is stable for highly inductive impedances for $\eta_c > 0$ and for highly capacitive impedance for $\eta_c < 0$ due to the long tail in that direction; the tail is reduced for a more truncated distribution; and stability is lost when $\eta_c = 0$.

Transverse Unbunched, Energy Spread

For a transverse impedance with no RF and a frequency spread arising from energy spread, the eigenvalue equation becomes

$$\bar{B}_\perp \left(\frac{\sigma_\delta [(k\omega_0 \pm \omega_\perp)\eta_c \mp \omega_\perp \xi]}{k\omega_0 \pm \omega_\perp - \omega} \right) = -iC \frac{IZ_\perp(k\omega_0 \pm \omega_\perp)}{E} \quad (15)$$

$\bar{B}_\perp(x)$ is dimensionless and for large x is approximately x^{-1} . Figure 2 shows plots of $1/B_\perp(x \pm i\epsilon)$ for the same distributions as in Fig. 1. The upper curve and lower curves are for the two signs in $x \pm i\epsilon$. Due to the symmetry of the impedance (assuming feedback is not included), the right hand side of Eq. (15) must be between both of the curves for stability, since even if it is on the stable side of both of the curves for one of the \pm signs in Eq. (15), it will be on the unstable side of both curves for the other sign of \pm (and the negative k) in that equation.

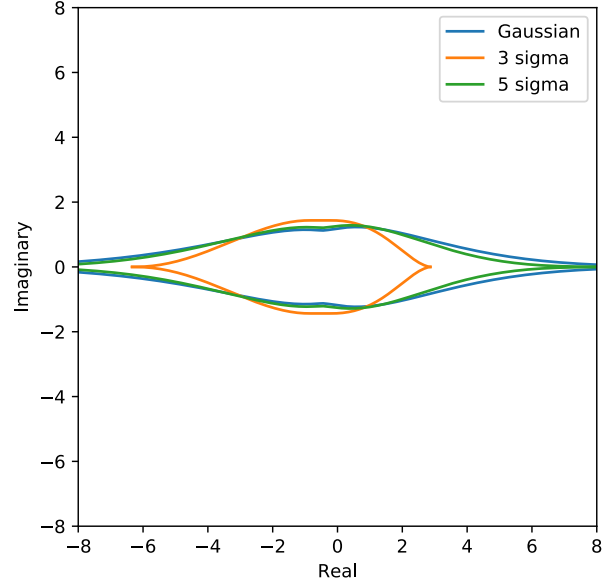


Figure 3: Stability diagrams for transverse motion and an unbunched beam where frequency spread arises from transverse tune spread. Tune shifts with amplitude are in opposite directions for the two planes.

Transverse Tune Spread

When variation in transverse amplitude is the dominant source of frequency spread, the formulations for bunched and unbunched beams are very similar. This is because it is the longitudinal motion that creates the distinction between bunched and unbunched beams, and that longitudinal motion is effectively integrated out.

When there is no RF and the energy spread gives a small contribution to the frequency spread (for instance when $(k\omega_0 \pm \omega_\perp)\eta_c \mp \omega_\perp \xi$ reaches its smallest value), the tune shift with transverse amplitude may become the dominant contribution to the frequency spread. In this case the eigenvalue equation takes the form

$$\bar{T}_y \left(\frac{\omega - k\omega_0 - \omega_y}{\alpha_{xy} - \omega\omega_x \xi_x \epsilon_x / c}, \frac{\omega - k\omega_0 - \omega_y}{\alpha_{xy} - \omega\omega_x \xi_x \epsilon_x / c} \right) = -iC \frac{IZ_\perp(\omega_y + k\omega_0)}{E} \quad (16)$$

There should be a \pm in various places in this equation, but that can be generally ignored, at least if there is feedback. The two arguments to \bar{T}_y take into account tune shift with amplitude in the two horizontal planes. If the tune shift with amplitude is negative, the tail of the stability diagram will correspond to an inductive impedance. If the tune shifts with amplitudes have opposite signs, the stability diagram will have tails in both directions (Fig. 3). The top and bottom curves are drawn for the two signs in $y/\bar{T}_y(x \pm i\epsilon, y \pm i\epsilon)$, and for stability the right hand side needs to be between the two curves due to the symmetry in the impedance.

The case of bunched beam with transverse tune spread is nearly the same as the transverse unbunched case. The first important difference is that an “effective impedance” is used, which is an integral or sum over the impedance times a weighting function. The weighting function is shifted by a frequency $\xi\omega_0/\eta_c$, breaking the symmetries mentioned earlier, meaning that we could have damped discrete modes that do not have corresponding growing discrete modes. The second important difference is that multiples of the synchrotron frequency enter in, as well as the amplitude dependence of those tune shifts, while the chromaticity terms are no longer present in the arguments to \tilde{T}_y . The chromaticity terms seen when there is no RF in Eqs. (15) and (16) are still present in the bunched case, they manifest themselves in the shift in frequency in the weight function when computing the effective impedance (and that frequency shift can be seen in Eq. (15)). The stability diagram is valid for individual modes for either the single or multi-bunch case. Thus, one solves the corresponding uncoupled problem for the eigenvalue Ω , and plots $\Omega - \omega_y - m\omega_z$ on the same diagram as

$$\tilde{T}_y \left(\frac{\Omega - \omega_y - m\omega_z}{\alpha_{yx} + m\alpha_{zx}}, \frac{\Omega - \omega_y - m\omega_z}{\alpha_{yx} + m\alpha_{zx}} \right) \quad (17)$$

evaluated at $\Omega = \omega + i\epsilon$ for ω real.

With coupling between modes with different m , this formulation can still be used because the integrals only depend on the distribution and the form of the tune shift with amplitude. One does not use a stability diagram: the coupled nonlinear equations are solved, and Eq. (17) is evaluated at an arbitrary complex Ω ; since m is different for each mode, the function must be evaluated at a number of different points. Chin *et al.* [6, 10] appear do this.

Longitudinal Tune Spread

Incorporating longitudinal tune spread in a bunched beam for a calculation for Landau damping presents the largest challenge for accelerator applications. But doing so is desirable since the longitudinal tune shift with amplitude can be the largest source of tune spread in the system. The challenge can be seen in the computation of $K(\Omega)$. This computation requires integrals of the form

$$\int \frac{[C_m^*(\mathbf{J})J_y \mathbf{m} \cdot (\partial\psi_0/\partial\mathbf{J})B_m(\mathbf{J}')Z(\omega)] J_m(\sqrt{2J_z\beta_z\omega})J_m(\sqrt{2J'_z\beta_z\omega})}{\Omega - \omega_y(\mathbf{J}) - m\omega_z(\mathbf{J})} d\mathbf{J} d\mathbf{J}' d\omega \quad (18)$$

This is the form for transverse modes, but the form for longitudinal modes is similar. The problem is the appearance of ω in the argument of the Bessel functions. The integrals of \mathbf{J} and \mathbf{J}' create a frequency-dependent weight function that multiplies the impedance. If the tunes in the denominator depend on J_z , then that weighting function depends on Ω , and their is not a single stability diagram that can be

drawn. One approach that can be taken is to expand the first Bessel function form small arguments [5]; unfortunately, this can get the high-frequency contribution for the effective impedance wrong. Initial experiments indicated that this approximation is optimistic [8]. Chin *et al.* [10] approach the difficulty with an additional summation.

For transverse instabilities, the tails in the stability diagrams are lost because modes with opposite signs of m generally have similar effective impedances (at least if the chromaticity is zero), but the tail of the stability diagram along the real frequency shift axis is in opposite directions for the two signs of m , so the resulting stability diagram has a very reduced area [8]. This problem is not present for longitudinal impedances.

REFERENCES

- [1] R. L. Pease, “Analysis of longitudinal accelerator instabilities,” *IEEE Trans. Nucl. Sci.*, vol. NS-12, no. 3, pp. 561–565, 1965, *Proc. 1st Particle Accelerator Conf. (PAC’65), Washington D.C., USA, Mar. 1965*. doi: 10.1109/TNS.1965.4323695. <https://www.jacow.org/>
- [2] A. G. Ruggiero and V. G. Vaccaro, “Solution of the dispersion relation for longitudinal stability of an intense coasting beam in a circular accelerator (application to the ISR),” CERN, Geneva, Switzerland, report CERN-ISR-TH/68-33, Jul. 1, 1968.
- [3] K. Hübner and V. G. Vaccaro, “Dispersion relations and stability of coasting particle beams,” CERN, Geneva, Switzerland, report CERN-ISR-TH/70-44, Aug. 25, 1970.
- [4] K. Hubner, A. G. Ruggiero, and V. G. Vaccaro, “Stability of the coherent transverse motion of a coasting beam for realistic distribution functions and any given coupling with its environment,” in *Proceedings, 7th International Conference on High-Energy Accelerators, HEACC 1969: Yerevan, USSR, August 27–September 2, 1969*, A. I. Alikhanian, Ed., also CERN-ISR-TH-RF/69-23, Akad. Nauk Armyanskoj. Inst. Fiz., 1970, pp. 343–325.
- [5] B. Zotter, “Longitudinal stability of bunched beams part ii: Synchrotron frequency spread,” CERN, Geneva, Switzerland, report CERN-SPS/81-19 (DI), Nov. 1981.
- [6] Y. H. Chin, “Hamiltonian formulation for bunched beam instabilities in the presence of betatron tune spread,” CERN, Geneva, Switzerland, report CERN-SPS-85-9 (DI-MST), May 28, 1985.
- [7] N. G. van Kampen, “On the theory of stationary waves in plasmas,” *Physica*, vol. 21, pp. 949–963, 1955, ISSN: 0031-8914. doi: 10.1016/S0031-8914(55)90413-4.
- [8] J. S. Berg and F. Ruggiero, “Stability diagrams for landau damping,” in *Proc. 17th Particle Accelerator Conf. (PAC’97), (Vancouver, Canada, May 1997)*, paper 7V030, IEEE, Piscataway, NJ, 1998, pp. 1712–1714. <https://www.jacow.org/>
- [9] J. S. Berg, “Beam transfer functions, stability diagrams, and schottky spectra for unbunched beams,” CERN, Geneva, Switzerland, report CERN-SL-97-049-AP, Dec. 7, 1999.
- [10] Y. Chin, K. Satoh, and K. Yokoya, “Instability of a bunch beam with synchrotron-frequency spread,” *Part. Accel.*, vol. 13, pp. 45–66, 1983.